Journal of Materials Chemistry B

Accepted Manuscript

This article can be cited before page numbers have been issued, to do this please use: A. K. S. Chandel, D. Kannan, N. Bhingaradiya, S. Singh and S. K. Jewrajka, *J. Mater. Chem. B*, 2017, DOI: 10.1039/C7TB00848A.

ROYAL SOCIETY OF CHEMISTRY

rsc.li/materials-b

Journal of Materials Chemistry B

View Article Online
DOI: 10.1039/C7TB00848A

ARTICLE

Dually crosslinked injectable hydrogels of poly(ethylene glycol) and poly[(2-dimethylamino)ethyl methacrylate]-b-poly(N-isopropyl acrylamide) as a wound healing promoter†

Received 00th January 20xx,
Accepted 00th January 20xx

DOI: 10.1039/x0xx00000x

www.rsc.org/

Arvind K. Singh Chandel[a], Deepika Kannan[b], Bhingradiya Nutan[a], Shailja Singh*[b] and Suresh K. Jewrajka*[a]

Abstract

Rapid gelation, low heat generation, biocompatibility, biodegradability, avoiding the use of small molecular weight gelator and high gel fraction are essential criteria for successful biomedical application of an injectable hydrogel. We have developed series of dually crosslinked injectable hydrogels of PEG and poly[2-(dimethylamino)ethyl methacrylate]-*b*-poly(N-isopropyl acrylamide) through extremely simple chemistry. Sequential reaction between PEG containing reactive termini and the copolymer provided chemically crosslinked hydrogels with gel fraction as high as 97-99% with gelation time 1-4 min in the physiological conditions. The gelation occurred with ca. 1 °C rise in temperature/g of the injectable solution, avoids formation of by-products and can be performed at temperature range of 20-37 °C. The hydrogels undergo hardening at physiological temperature as confirmed by the rheological experiments. The gelation time, water swelling, mechanical properties and the degradability of the hydrogels depend on the PEG to copolymer ratio in the injectable solution. Rheological behaviour of the fully hydrated hydrogels showed desirable mechanical property for soft tissue regeneration. The hydrogels exhibited blood compatibility and retained the viability of HepG2 cells with time. Platelets adhesion and aggregation followed by fibrinogen adsorption ability makes these hydrogels suitable for wound healing application.

Introduction

Injectable and implantable hydrogels have attracted wide attention due to their applications in tissue engineering,[1-4] cell delivery, wound healing,[5-11,] and drug delivery.[12-19] Physical gelling,[3,13] chemical gelling,[16-18] and both physical and chemical gelling[20-24] were reported. Thermo-induced gelation of polymers is an attractive way for in situ hydrogels formation.[25-32] Notably, random copolymers of poly(N-isopropyl acrylamide) and poly(acrylic acid) [Poly(NIPAAm-co-AA)],[29] triblock copolymers of poly(ethylene glycol) and poly(lactic acid-co-glycolic acid),[30] and some natural polymers[31] showed sol-gel transition when heated above their gel point. The sol-gel transition is realized due to the rapid dehydration and hydrophobization of the temperature responsive polymers. Garbern et al. reported pH- and temperature-responsive copolymers for the in situ formation of hydrogels.[32]

For successful tissue regeneration application, the degradation rate of a biocompatible hydrogel should match with the tissue regeneration rate.[33,34] The mechanical property of a hydrogel should also be similar to that of the surrounding tissue.[35,36] The topography of hydrogel is also crucial.[37] Hydrogel systems which avoid the formation of by-products and show high gel fraction under the physiological condition is desirable for direct application. The generation of heat should also be minimized during in situ gelling process to avoid morbidity and tissue necrosis surrounding the injection site. Optimization of initiator concentration and light intensity in the photo-induced polymerization minimizes the undesirable temperature rise.[38] A problem of physically crosslinked gels is the high water swelling which lowers the mechanical property. Previously, we reported the preparation of mechanically strong amphiphilic conetwork gels with tuneable water swelling and degradability by crosslinking of tertiary amine containing hydrophilic (co)polymers with halide terminated poly(caprolactone) (PCL) in organic solvent.[39-42]

As regards to injectable hydrogels, chemical gelation and temperature induced hardening (dual gelation) minimize the problem of physically crosslinked hydrogels.[20-24] For example; Lee et al. reported both chemical and physical gelling of PNIPAM-based copolymers. The NIPAM groups provided physical gelling and the acrylate part of the copolymer undergoes chemical gelling with pentaerythritol tetrakis 3-mercaptopropionate through Michael addition reaction.[22] This hydrogel showed improved elastic property than the hydrogels obtained by physical gelation. The water swelling of the hydrogel was also reduced compared to physically

[a]*academy of Scientific and Innovative Research-CSIR, Central Salt and Marine Chemicals Research Institute G. B. Marg, Bhavnagar, Gujarat 364002, India*
[b]*Department of Life Science, Shiv Nadar University, NH91, Tehsil Dadri Gautam Buddha Nagar, Uttar Pradesh–201314, and Special Centre for Molecular Medicine, Jawaharlal Nehru University, Delhi – 110067, India*
**Email -skjewrajka@csmcri.res.in or shailja.jnu@gmail.com*
† Electronic supplementary information (ESI) available

crosslinked hydrogels. PNIPAM-based thermo-gelling of macromonomers with a hydrolysable lactone ring, epoxy pendant groups and a biodegradable diamine-functionalized poly(amido amine) cross-linker were synthesized and combined to obtain in situ hydrogel.[23] Thermo-responsive physical gelation of the PNIPAM-based copolymer was combined with chemical ligation for the formation of in situ hydrogel.[24] Earlier, the gelation time was successfully lowered or tailored through rapid chemical reactions.[7,22] The degradation mechanism of the hydrogels was also controlled for practical applications.

We hypothesized that the criteria mentioned here for a hydrogel system in tissue regeneration process could be met if a water soluble copolymer with lower critical solution temperature (ca. physiological temperature) undergoes rapid chemical crosslinking with a biocompatible water soluble macromolecule containing reactive termini linked with degradable moiety. Based on our hypothesis, we proposed in situ mild chemical gelation of pH and temperature-responsive poly[(2-dimethylamino)ethyl methacrylate]-*b*-poly(N-isopropyl acrylamide) (PDMA-b-PNIPAM) by PEG (containing activated chloride termini linked with degradable ester) through rapid nucleophiplic substitution reaction. We have demonstrated that the aqueous solutions (pH 7.4, 25-37 ^{o}C) of PDMA-*b*-PNIPAM and reactive PEG after co-injection gave hydrogel within 1-6 min depending on the composition of the injectable solution and gelation temperature. The system showed ca. 1 ^{o}C rise of temperature/g of injectable solution. The in situ formed hydrogels were degradable and exhibited hardening effect at physiological temperature. The degradation behaviour and the responsive property of the hydrogels could be adjusted by varying the ratio of PDMA-*b*-PNIPAM to reactive PEG. These hydrogels could encapsulate cells and exhibited platelet adhesion/aggregation activity which is useful for vascular wound healing application.

Experimental

Materials

PEG (Mn= 4000 g/mol), 4-(chloromethyl) benzoyl chloride (Cl-Bz-Cl, 98%), and phosphate buffer (PBS, 98%) were procured from Sigma Aldrich. HepG2 (NCCS, Pune, India), all the salts, HEPES, (Glucose), bovine serum albumin (BSA), DMSO, Triton X-100, ADP (10mM), Skimmed milk, anti-FGA produced in rabbit, anti-rabbit IgG HRP conjugated, were purchased from Sigma-Aldrich (St. Louis, MO, U.S.A). Dulbecco's modified Eagle's medium (DMEM), fetal bovine serum (FBS), penicillin-streptomycin antibiotic solution, Trypsin-EDTA, 3-(4,5-dimethyl- 2-thiazolyl)-2,5-diphenyl-tetrazolium bromide (MTT), Trypan Blue, Propidium Iodide (PI) and Hoescht 33342 (H33342) were from Life Technologies Ltd (CA, USA). LDH assay-CytoTox 96® Non-Radioactive Cytotoxicity Assay from Promega Corp. (WI, USA), TMB (10X) from Himedia Laboratories (Mumbai, India). The 96 well polystyrene plates, 24 well polystyrene plates, and 25 cm2 tissue culture flasks were purchased from Nunc, Thermo Fisher Scientific (NY, USA). Tyrode's buffer (134 mM NaCl, 12 mM NaHCO3, 2.9 mM KCl, 0.34 mM Na_2HPO_4, 1 mM $MgCl_2$, 10 mM HEPES, 5 mM Glucose, set pH 7.4, freshly added BSA 3 mg/ml) was prepared and used. Activated halide terminated PEG (Cl-PEG-Cl) was synthesized by the esterification reaction (supporting information). PDMA-*b*-PNIPAM copolymer with GPC derived molecular weight ca. 25000 g/mol (PDI=1.30) and ^{1}H NMR spectroscopy derived molecular weight ca. 32000 g/mol (DMA: NIPAM=32:68 mol/mol) was synthesized by the reversible addition fragmentation (RAFT) polymerization (Fig. S1, ESI†).[39]

Injectable hydrogels system

Lyophilized Cl-PEG-Cl (ESI†) powder was dissolved in PBS (7.4 pH, 0.5 g/mL) at 25 ^{o}C. The PDMA-*b*-NIPAM was also solubilized in PBS (7.4 pH, 0.1 g/mL) by stirring at 25 ^{o}C. The two solutions were mixed in different proportion separately in glass vials. After vigorous hand shaking for 10 sec, the mixed solutions were kept at temperature 25 ^{o}C or 37 ^{o}C. The gelation time of the prepolymer solutions was noted visually when no gel flow occurred. The gelation time was also determined by the rheological experiments (vide infra). The reaction mixture is easily injectable through the hypodermic syringe. The PDMA-*b*-NIPAM to Cl-PEG-Cl ratio (w/w) in the mixture was varied and the total polymer concentration was maintained to 12% (w/v) by the addition of PBS to avoid dilution effect on the rheological property. HG-1, HG-2, HG-3, and HG-4 hydrogels with different PEG to PDMA-*b*-PNIPAM ratio (w/w) were obtained by the above procedure (Table. S1, ESI†).

Characterizations of hydrogels

The hydrogels were characterized by the ^{13}C NMR spectroscopy and FT-IR spectroscopy (ESI†). Sol fraction, water swelling, and degradation experiments were performed using standard protocols (ESI†). [37,39-42,21,23]

Lower critical solution temperature (LCST) of the hydrogels was determined on a DSC Mettler Toledo Instrument. The freshly prepared hydrogels were allowed to undergo hydration in contact with Millipore water and kept at 10 °C for 1 h. The hydrogels were then put in the DSC Pans and were sealed. In the DSC measurements, the samples were run at 10 ^{o}C for 1h to obtain a stable baseline. After that, the samples were heated up to 60 °C with a scanning rate of 1 °C/min. The same experiment was performed with PDMA-*b*-PNIPAM copolymer solution (12%, w/v in water) for the purpose of comparison.

Rheological properties and evaluation of gelation time

The rheological properties were evaluated with a Physica MCR 301 rheometer (Anton Paar) using pp50 (Diameter 49.973 mm) probe. The gap between the probe and the plate was maintained at 0.1 mm for time sweep and frequency sweep experiments. The gap was maintained to 0.2 mm for the fully water-swollen hydrogels to perform temperature sweep experiment. For time sweep experiment, storage modulus (G') and loss modulus (G'') were monitored as a function of time at 25 ^{o}C and 37 ^{o}C respectively. The experiments were conducted at constant frequency of 1 Hz and strain 1% (linear viscoelastic region, Fig. S2, ESI†). Mixtures of Cl-PEG-Cl (50% w/v in PBS pH 7.4) and PDMA-*b*-PNIPAM (10% w/v in PBS pH 7.4) were taken in a syringe (total 12% w/v) and was injected (300 µL) in between parallel plate geometry (50 mm). The time lag between mixture preparation and injection was 15-20 sec. The sol-to-gel point i.e. the gelation time was defined as the time at which G' is equal to the G'' at fixed temperature.

Frequency sweep test was performed at 37 ^{o}C by the scanning in the range of 0.1 to 100 rad/s. The frequency sweep experiment was performed after 30 min of the hydrogels formation at 37 ^{o}C. For temperature sweep experiment, G' and G'' were monitored as a function of temperature in the range of 20–50 ^{o}C at the heating rate of 0.1 ^{o}C/s. Fully water-swollen hydrogel samples were used for the temperature sweep measurements, since the hydrogels remain in fully water-swollen state in practical use.

Hemocompatibility, cytocompatibility, cell Proliferation and cell morphology

Hemocompatibility of the hydrogels was determined by the hemolysis assay with human blood cells. The MTT assay was performed with HepG2 cells (ESI†).

Cell proliferation assay was performed by Trypan blue method.[43] Cells were grown in 25 cm^2 polystyrene tissue culture flasks in 5% CO_2 atmosphere at 37 °C with Dulbecco's modified Eagle's medium (DMEM) containing 10% fetal bovine serum and 1% penicillin-streptomycin solutions. Hydrogels (100 µL each by direct injection) were prepared and saturated overnight at 37 °C with 0.01M PBS and seeded with $1x10^4$ cells per well in a 96-well plate and incubated in CO_2 incubator at 37 °C for 6, 12, 24 and 48 h respectively. Cells seeded on polystyrene tissue culture plates for the same time periods were used as a control. After the desired time period, cells (from sample and control) were trypsinized and diluted with trypan blue (1:1). 10 µL of the dilution was loaded in the haemocytometer to count the live and dead cells. The experiment was performed in triplicates. Percentage of the live cell was calculated for each time period with the respect to control samples.

Representative HG-2 hydrogel was saturated with DMEM overnight at 37 °C. HepG2 cells were seeded (50,000 cells) in 35 mm^2 culture dish with the hydrogel. Cells seeded on the culture dish without hydrogel was used as the control. After 24 h of incubation cells were washed with 0.01M PBS thrice. Nuclei were stained with (H33342) Hoescht 33342 (1:1000) along with Propidium iodide (1:1000) to stain cells undergoing apoptosis/necrosis. Cells were stained for 15 min and washed twice with 0.01 M PBS. Visualization was then done in Nikon Ti2 eclipse microscope.[43]

Platelet isolation, platelet adhesion, and platelet activation

Human whole blood was collected in citrated tubes to isolate platelets as explained by Watson with few alterations.[44] Blood was centrifuged at 200 g (no brake) for 20 min to separate the plasma rich platelets (PRP) from erythrocytes. PRP was further centrifuged at 200g (no brake) for 10 min to remove remnant RBC. PRP was again centrifuged at 2000 g for 10 min. The supernatant was collected as plasma poor platelet (PPP) while the pellet rich in platelets was re-suspended in Tyrode's buffer and counted in the haemocytometer. To determine the platelet density different concentration of platelets (0-300$x10^3$) 100 µL each were prepared in Tyrode's buffer as diluent. These concentrations were used to plot the standard curve. 70 µL of each concentration was treated with 2%, (v/v) Triton X-100 in 0.01 M PBS buffer for 30 min at 37°C. 50 µL of the lysed platelet solution was transferred to a 96 well plate and incubated with 50 µL of LDH substrate for 30 min at 37 °C. Reaction was stopped with 50 µL stop solution. The absorbance was noted at 490 nm.

The release of LDH was estimated to evaluate the effect of hydrogel on platelet activation. Platelets with concentration (0-100 $x10^3$) were allowed to adhere on representative HG-2 hydrogel saturated with 0.01 M PBS overnight.[45] Tyrode's buffer was used as a diluent. After hour incubation at 37 °C buffer was removed and the adhered platelets were lysed with 0.01M PBS containing 1%, (v/v) Triton X-100 for 30 min at 37°C. A 50 µL of the lysed platelet solution was incubated with 50 µL of LDH substrate for 30 min at 37°C. Reaction was stopped by adding 50 µL of stop solution. The absorbance was noted at 490 nm.

Activation of the platelets was measured based on the amount of LDH enzyme released. Platelet concentrations ($50x10^3$ and $100x10^3$) were prepared in Tyrode's buffer and stimulated with 20 µM ADP at 37 °C for 15 min.[45] Non-ADP platelet dilutions (resting) were used as control. Followed by stimulation, platelet suspensions were centrifuged at 2000g for 15 min at room temperature. Supernatant was collected and LDH enzyme activities were assayed as described above. For the HG-2 hydrogel, platelets in above mentioned concentration were allowed to adhere on 0.01 M PBS saturated hydrogel. For the assessment of the platelet activation, one set was induced with 20 µM ADP while the non-ADP platelet dilutions on the hydrogel were used as a control. Upon centrifugation, supernatant was subjected to LDH assay.

Fibrinogen adsorption

To assess the adsorption of plasma derived fibrinogen on the hydrogel, 0.01M PBS saturated HG-2 hydrogel was incubated with platelet poor plasma (PPP) overnight.[46] The fibrinogen in PPP was coated on the gel overnight at 4 °C. Gel without PPP was used as control. Also fibrinogen coated on polystyrene 24 wells plate was used as positive control while well without PPP was used as reference control. The fibrinogen adsorption was then assayed by ELISA. HG-2 hydrogel samples were rinsed (3x5min) with 0.01 M PBST (0.05% tween-20), blocked for 1 h (5% skimmed milk in 0.01M PBS), rinsed with 0.01M PBST (3x5min), incubated in primary antibody for 1 h at room temperature (anti-FGA produced in rabbit 1:1000), rinsed with0.01M PBST (3x5min), incubated in secondary antibody for 1 hr (anti-rabbit IgG HRP conjugated 1:10000), and rinsed with 0.01M PBST (3x5min). Solution was transferred to 96 wells plate and incubated with substrate (3, 3', 5, 5'-Tetramethyl benzidine) (1xTMB) for 30 min. at 37 °C in dark. The absorbance was read at 450 nm. Platelet adhesion on a representative hydrogel HG-2 was visualized by the scanning electron microscopy (SEM, ESI†).

Results and discussion

Dually corsslinked injectable hydrogels from reactive prepolymers

Injection of the aqueous (PBS, pH 7.4) mixture of of PDMA-*b*-PNIPAM (Mn=27000 g/mol, PDI=1.28) and Cl-PEG-Cl (Mn=4000 g/mol, PDI=1.21) gave chemically crosslinked hydrogels (Scheme 1, part A). Visual observation indicated that the gelation time varied from ca. 1.2-3.5 min at 37 °C depending on the PDMA-*b*-PNIPAM to Cl-PEG-Cl ratio (w/w). The fast nucleophilic substitution reaction between PDMA-*b*-PNIPAM and Cl-PEG-Cl in the physiological conditions is due to the reactive nature of the tertiary amine of the copolymer towards the activated chloride termini of the PEG. This gelation reaction avoids formation of by-product owing to the quaternization of the amine groups of the copolymer (Scheme 1, part B).[47] The tertiary amine groups of the PDMA exclusively react with Cl-PEG-Cl as confirmed by the model gelation reaction (ESI†). Gelation did not occur by mixing solutions of PNIPAM homopolymer and the telechelic PEG while the mixture of PDMA homopolymer and the telechelic PEG solutions yielded hydrogel instantaneously. The reaction was performed at 25 °C which is below the LCST of PNIPAM. Usually, the nitrogen atom of PNIPAM chains is inactive towards the nucleophilic substitution reaction.

Injection of 1 g of solution mixture containing Cl-PEG-Cl and the copolymer (1:1, w/w) yielded hydrogel with temperature rise as low as ca. 1 °C (ESI†), confirmed experimentally. The approximate MM2 simulation also showed low degree of temperature rise (ESI†). This temperature rise is well below the acceptable limit for in situ application.[38] Furthermore; our gelation can be performed well below the physiological temperature with reasonable rate which is

Journal of Materials Chemistry B

View Article Online
DOI: 10.1039/C7TB00848A

beneficial to overcome heating effect if any. Table 1 shows the abbreviations, compositions, observed gelation time, equilibrium water swelling, and sol fraction of HG-1 to HG-4 hydrogels.

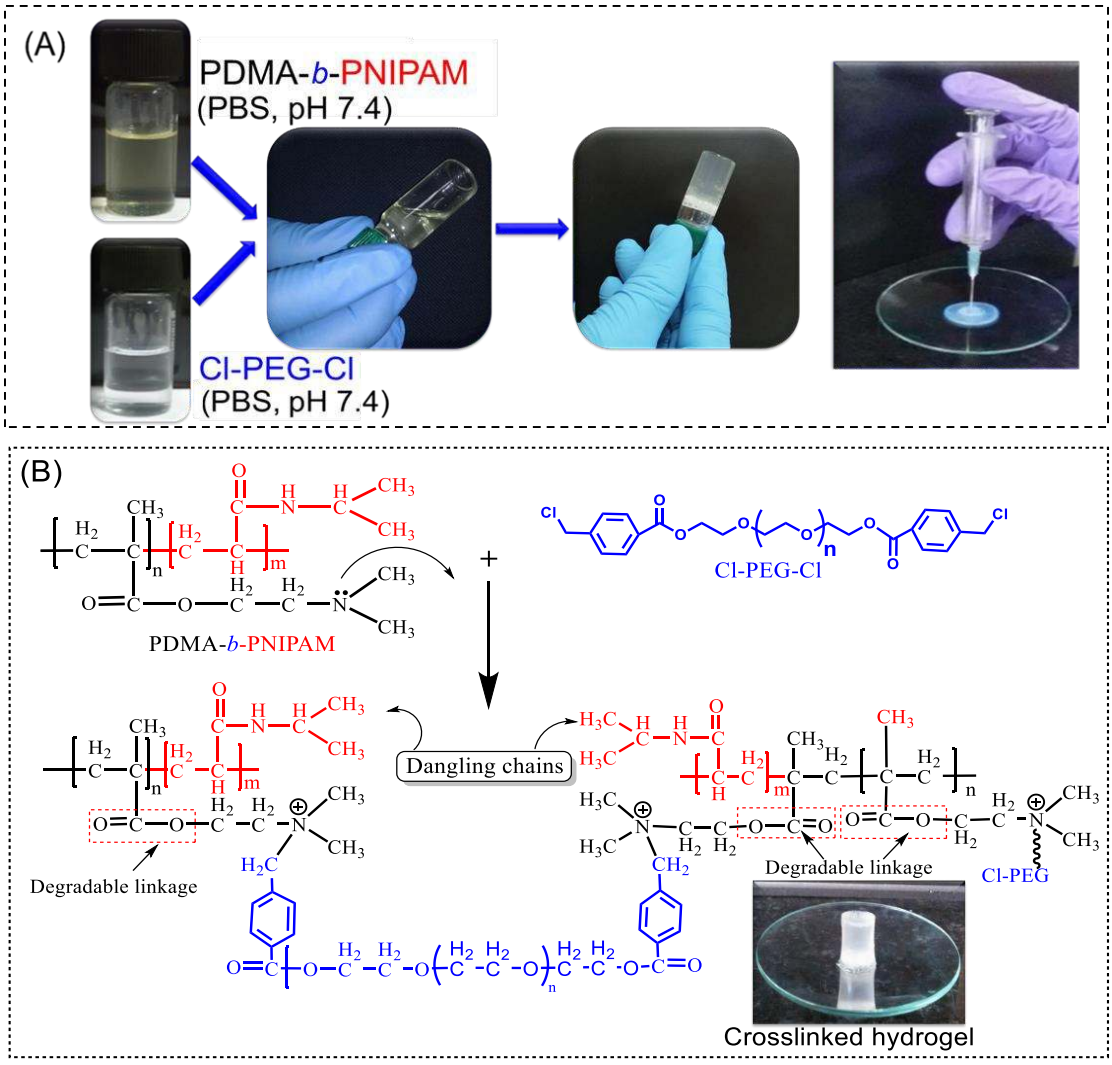

Scheme 1. (A) Schematic representation of in situ (injectable) hydrogel formation, and (B) gelation mechanism.

The sol fractions of the hydrogels were 2-6% (w/w) in DMF and 1-2% (w/w) in PBS (pH 7.4) at 37 °C. These hydrogels remained stable in the temperature range 0 °C to >70 °C in PBS. The FT-IR and solid state ^{13}C NMR spectra confirmed the formation of tri-component hydrogels (Fig. S3, ESI†).

Table 1. Composition, observed gelation time, sol fraction, and equilibrium water swelling (S_w) of the hydrogels.

Hydrogel	CL-PEG-Cl/ PDMA-*b*-NIPAM (w/w)	Equilibrium water swelling (%) at pH 7.4, 37 °C, (%)	Gelation time (min) (25 °C/37 °C)	Sol fraction (% , w/w)	
				DMF	PBS
HG-1	25/75	2650	8.5/3.5	6.1 (±0.78)	3.7 (±0.78)
HG-2	50/50	790	7.2/2.3	2.3 (±0.47)	1.3 (±0.17)
HG-3	60/40	1070	6.3/1.8	2.0 (±0.25)	1.1 (±0.20)
HG-4	70/30	1290	4.2/1.2	2.1 (±0.22)	1.1 (±0.21)

Temperature- and pH-responsive property of the hydrogels

The values of equilibrium S_w of the hydrogels increased with increasing PEG content, except HG-1 which showed higher value (Table 1). The exceptional result obtained with HG-1 is attributed to its lower degree of crosslinking as well as higher porosity as confirmed by the rheological and SEM analyses (vide infra). The gelation reaction was performed with relatively little amount of Cl-PEG-Cl (25%, w/w) with PDMA-*b*-PNIPAM for the preparation of HG-1. The lowering of the ratio between nucleophilic tertiary amine groups to the activated chloride groups caused lowering of crosslinking density in this hydrogel. The chemical crosslinking was performed by reacting Cl-PEG-Cl (25-75%, w/w or 0.025–0.075 mol) and PDMA-*b*-PNIPAM (with DMA groups in the range 0.06-0.18 mol). Hence, besides thermo-responsive PNIPAM dangling chains, the hydrogels also contain pH-responsive PDMA chains and showed pH- and temperature-responsive swelling (Fig. S4 and relative

discussion, ESI†). These hydrogels exhibited hysteresis during cyclic heating-cooling process in the water swelling behaviour (Fig. S5, ESI†). The effect of PNIPAM and PDMA on the temperature- and pH-responsive properties of gels was reported elsewhere.[39]

Effect of composition and temperature on the gelation time, rheological property and LCST of the hydrogels

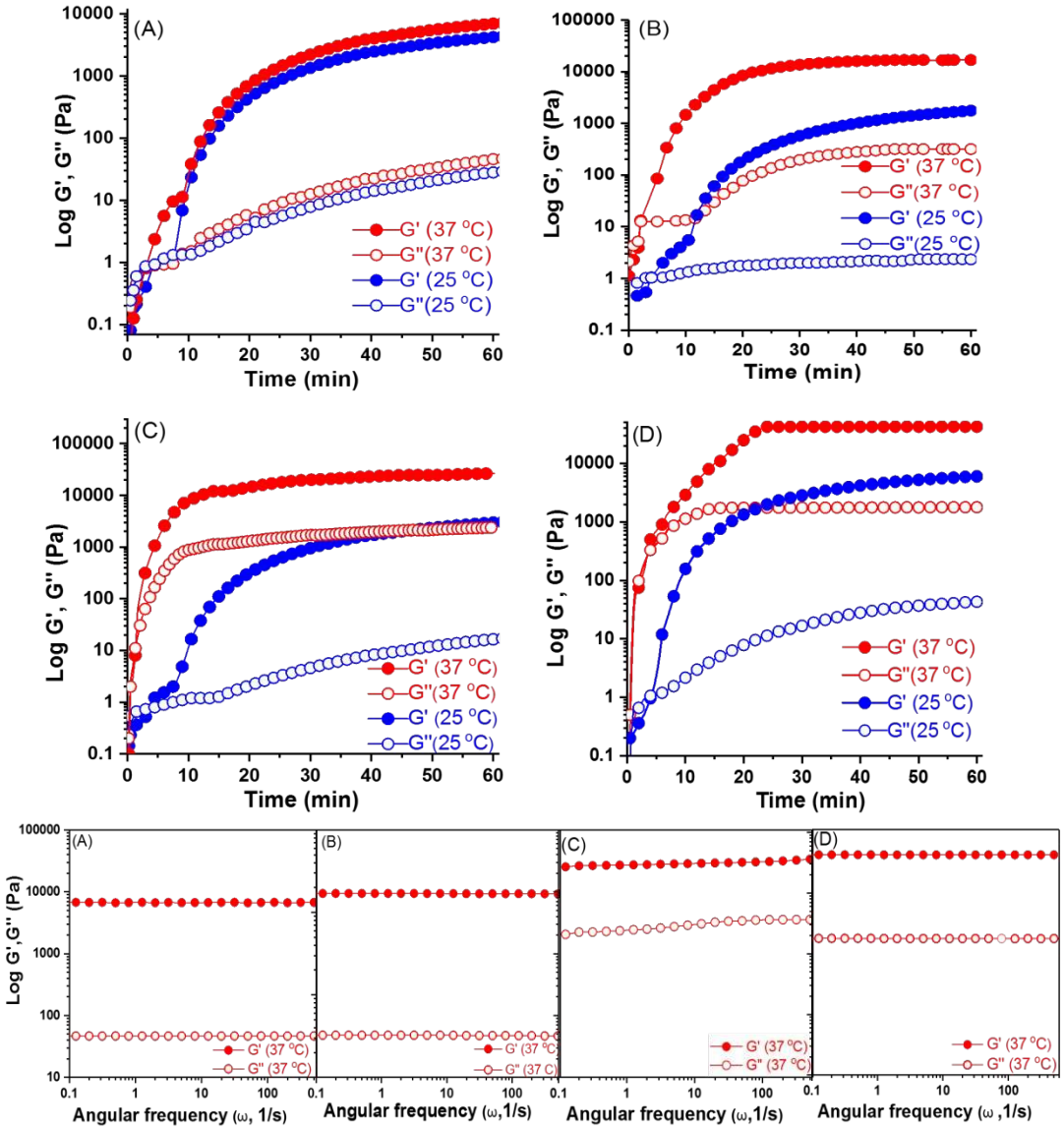

Figure 1. Oscillatory time sweep experiments (1% shear strain and at frequency 1 Hz) of the (A) HG-1, (B) HG-2, (C) HG-3, and (D) HG-4 hydrogels at 25 °C and at 37 °C respectively. The hydrogels were formed by the injection of aqueous solutions (varying proportion) of PDMA-b-PNIPAM (10%, w/v) and Cl-PEG-Cl (50%, w/v) in the rheometer. The total concentration was 12% (w/v). The solutions pH was 7.4 (in PBS). Lower panel: Oscillatory frequency sweep experiments at 37 °C with the hydrogels. The frequency sweep experiments were performed after 60 min of gelation.

The time-dependent changes in the storage modulus (G') and loss modulus (G'') of the hydrogels were monitored by the oscillatory time sweep experiment at the constant frequency (1 Hz) and temperatures 25 °C and 37 °C (Figure 1A-D). The value of G'' was initially higher than that of the G'. There is an intersection between the G'-time and the G''-time plots in a short reaction time (Fig. S6, ESI†). This indicates gelation (seizing of flow). It was also seen that the gelation time decreased from HG-1 to HG-4 system which is attributed to the enhancement of the concentration of Cl-PEG-Cl in the aqueous mixture (Table S2, ESI†). The bimolecular collision frequency between the tertiary amine and the activated halide was enhanced from HG-1 to HG-4 system. Furthermore, the gelation time of the mixtures was 2.5-7.5 min at 25 °C. The gelation time was lowered to 1-4 min with a steep rise of G'' within 10 min at 37 °C (Fig. S6 and Table S2, ESI†). This is attributed to the enhanced

rate of nucleophilic substitution reaction as well as association of the NIPAM groups owing to the development of hydrophobic character at >32 °C (vide infra). The G' remained almost unaltered after 25 min of operation at both the temperatures.

The storage modulus increased in the order for hyrogels as HG-1<<HG-2<HG-3<HG-4 (Figure 1 A-D and Table S2, ESI†). This order of modulus is due to increasing effect of degree of crosslinking which enhanced the hardening effect. Usually, the G'' values of the hydrogels were higher at 37 °C compared to that of 25 °C (Table S2, ESI†).

The angular frequency sweep experiment was performed after 60 min of time sweep experiment at 37 °C (Figure 1, lower panel). The values of G' and G'' remained almost unchanged with increasing frequency while the value of G'' remained much lower than that of G'. These values indicate stability of the hydrogels in their water-swollen state.

The abovementioned rheological experiments were performed at definite concentration of the prepolymers to avoid dilution effect on the gelation time. On the other hand, hydrogels usually remain in the fully hydrated state for practical use owing to the presence of plenty of fluid in the body system. Hence, we performed temperature sweep experiment with premade (after about 60 min) and fully water-swollen hydrogels at the constant frequency (Figure 2, A-D). The modulus increased with increasing temperature. This effect was more pronounced at temperature range of 32-40 °C. It may be noted that the premade hydrogels used herein were fully hydrated and thus exhibited lower modulus than that of the in situ hydrogel systems as described above (Figure 1).

The digital photographs (Figure 2E) show that the degree of opacity of a representative HG-2 hydrogel increased with the increasing temperature from 15 °C to 37 °C. The degree of opacity was maximum at ca. 32 °C which is the LCST of PNIPAM. This indicates increasing degree of de-swelling and phase separation of the PNIPAN chains in the water swollen state at temperature range 32-37 °C. The LCSTs of the water-swollen hydrogels were quantitatively determined by the DSC experiment. The thermograms (Figure 2F) show endotherms for all the hydrogels as well as for the aqueous solution of PDMA-*b*-PNIPAM. The minima of the endotherms (LCST) appear at ca. 31 °C during the controlled heating process. The PNIPAM homopolymer shows sharp transition with abrupt heat uptake.[48] However, the phase transition in our hydrogels as well as PDMA-*b*-PNIPAM slowed down compared to that of neat PNIPAM owing to enhanced hydrophilicity of the

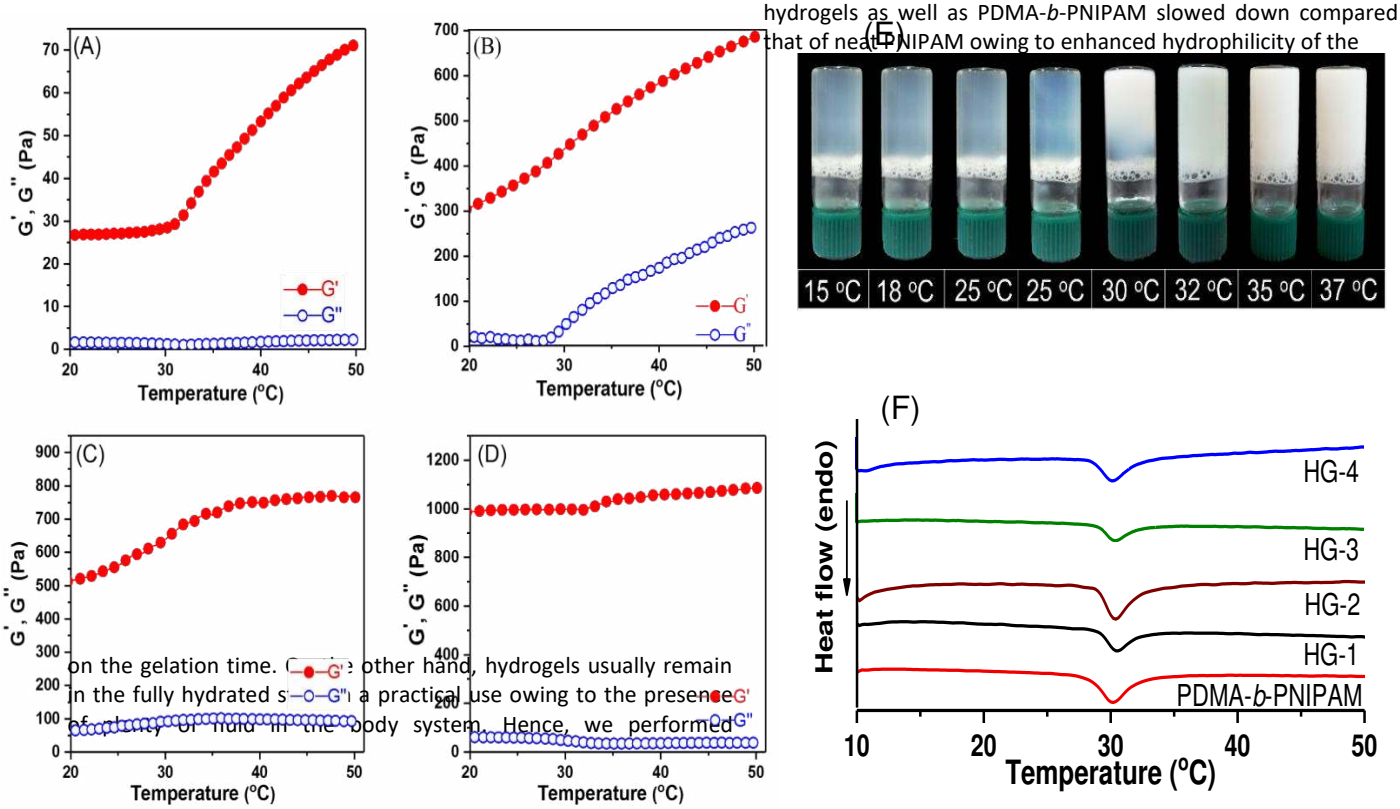

Figure 2. Modulus vs. temperature plots of (A) HG-1, (B) HG-2, (C) HG-3, and (D) HG-4 hydrogels. The premade hydrogels were fully hydrated to reach equilibrium swelling. The water-swollen hydrogels were subjected to rheological testing at frequency 1 Hz. Photographs (panel E) showing relative transparency of a representative water-swollen HG-2 hydrogel at different temperature. The photographs were taken after equilibrating the hydrogel in each temperature for 4 min. DSC thermograms (F) of water swollen hydrogels showing LCST.

hydrogels and the copolymer. The PNIPAM in the hydrogels remained as dangling chains since the crosslinking took place with the amines moieties of PDMA part of the block copolymer. Hence, the energy required for effecting the conformational changes is not affected by the presence of PEG chains or its conformation. Therefore, the effect of PEG and the extent of crosslinking on the LCST of the hydrogels is negligibly small. The hydrogel with low crosslinking density and obtained by the polymerization of NIPAM and N,N′-methylenebisacrylamide showed less changes on LCST due to the conformational changes of only PNIPAM chains.[49] However, when the relatively, high molecular weight PEG is directly connected to PNIPAM chains through crosslinking, the overall LCST increased compared to the above mentioned system. On the other hand, interconnected hydrophobic polymer chains negatively influenced the LCST of PNIPAM as reported by Kali et al.[48]

Morphology and degradation behaviour of the hydrogels

Surface and the cross-sectional SEM images (experimental details, ESI†) of the representative hydrogels showed porous nature (Figure 3A-C). The average diameters of inner pores of HG-1, HG-2 and

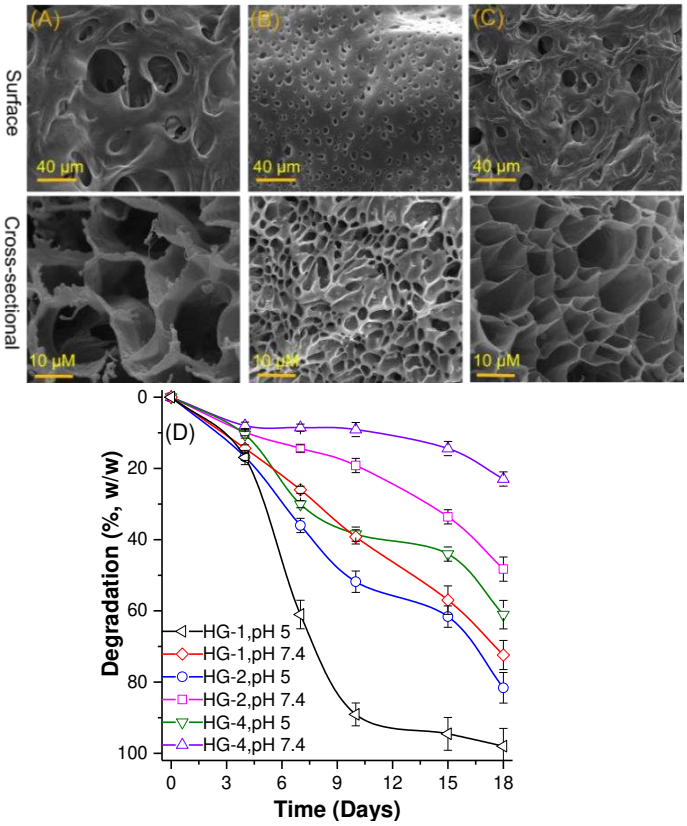

Figure 3. SEM images of (A) HG-1, (B) HG-2, and (C) HG-4 hydrogels. Plots in Figure D: Hydrolytic degradation profiles of the hydrogels at two different pH and at 37 °C.

HG-3 hydrogels were 13, 3.9 and 10 µm respectively. Furthermore, the pores were more uniform with increasing PEG content in the hydrogels due to the increase of crosslinking. The development of pores is due to the crosslinking during chemical reaction. The pore structure retained due to the freezing of the network structure during lyophilisation process which avoids pore shrinking.

The hydrogels undergo degradation in aqueous environment (Figure 3D). The degradation was catalysed in mildly acidic environment. The degradation of the hydrogels is attributed to the hydrolysis of the ester groups situated at beta position of the quaternized nitrogen atom (dotted line, Scheme 1B). Presence of positively charged nitrogen facilitated the hydrolytic cleavage by the lowering of electron density on the carbonyl carbon of the ester groups. Thus, hydrolysis of the ester bonds of PDMA is responsible for the degradation of the hydrogels.[50] Figure 3D shows that the rate of degradation specifically follows the order, HG-1>>HG-2>HG-3>HG-4. Since, the nature of cleavable linkage is the same; the extent of crosslinking and the degree of water swelling were the major factors which caused such difference in degradation pattern. Hence, the extent degradation may be controlled by adjusting the PEG to copolymer ratio in the injectable solution.

Blood contact property, cell viability, cell proliferation and cell morphology

The hydrogels showed 2-8% hemolysis whereas total hemolysis occurred with the positive control (Figure 4A). This indicates ability of the hydrogels in the direct blood contact application. Indeed, <20% hemolysis is considered to be hemocompatible.[51] The viability of cells on the hydrogels was similar (within the error bars) to control. The live cell attachment increases with time for the representative HG-2 and HG-4the hydrogels. This indicates good cytocompatibility and cell encapsulation property of the hydrogels (Figure 4B).

Cellular proliferation was observed with representative HG-2 and HG-4 hydrogels by trypan blue live-dead assay. The hydrogels showed proliferation of HepG2 cells with time without cell dead (Figure 4C). The cell morphological study was performed with H33342 and PI staining. This study indicates any apoptotic or necrotic behaviour or growth arrest in the cell cycle. Usually HepG2 cells being an epithelial lineage and exhibits polygonal shape with adherence in discrete patches. A representative HG-2 hydrogel showed desired polygonal shape aggregated morphology (Figure 4E) similar to the control cells (Figure 4D). Furthermore, all the cells grown on the hydrogel (Figure 4E') showed intact nuclear staining devoid of any granulation or fragmentation as observed for control one (4D'). Further, cells treated with the hydrogels remains healthy with the enhancement of size compared to that of control. This indicates the ability of the hydrogel for the use in tissue regeneration.

Platelet adhesion, activation and fibrinogen adsorption activity

Platelet and fibrinogen adhesion is one of the important indicator for wound closing.[52] Platelets adhesion experiments on a representative HG-2 hydrogel was undertaken in three different platelets concentrations (25 x 10^3, 50x10^3 and 100x10^3 platelets/µL, freshly isolated) (Fig. S7, ESI†).

Journal of Materials Chemistry B

View Article Online
DOI: 10.1039/C7TB00848A

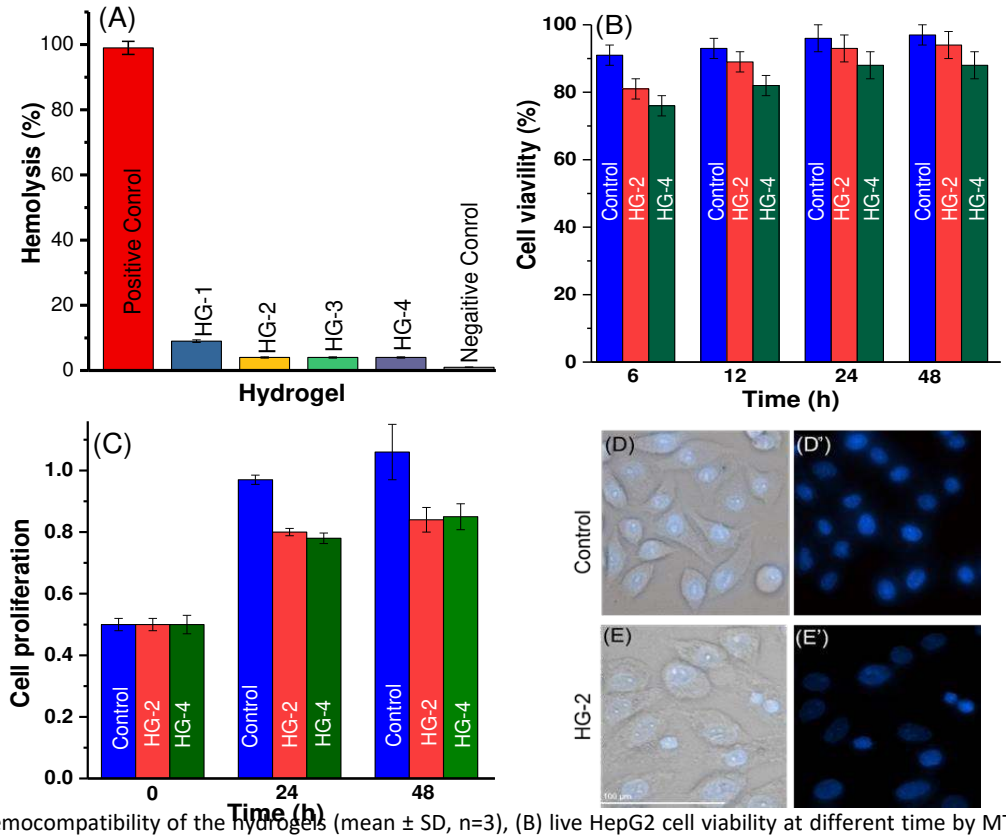

Figure 4. (A) Hemocompatibility of the hydrogels (mean ± SD, n=3), (B) live HepG2 cell viability at different time by MTT assay, and (C) Bar diagrams showing live HepG2 cell proliferation on representative HG-2 and HG-4 hydrogels. Cellular morphology (images D, and E cell growth, and images D' and E' nucleus structure) of HepG2 cells observed by Nikon Ti2 (40X magnification) eclipse microscope after 24 h treatment with HG-2 hydrogel. Images D and D' are for control experiment on polystyrene tissue culture plate and E and E' are for the HG-2 hydrogel.

The release of LDH enzyme from the lysed platelets was estimated where defined concentrations of platelets served as standards. An almost linear regression line shows the increase in absorbance value relative to the LDH release with respect to defined platelet concentration (Figure 5A). The density of platelet adhered on the hydrogel were significant, indicating its wound closure ability (Figure 5B). The SEM images (Figure 5, Images C and D) shows that the isolated platelets confined to dendritic morphology with variable length pseudopodia on the coverslip (control). However, the isolated platelets on HG-2 were adhered and showed aggregated morphology rather than fully spread or dendritic appearance (Figure 5, images E and F). This is consistent with the results of Figures 5 A and 5B. Presumably, enhanced hydrophobic character of the hydrogel at physiological temperature together with crosslinked porous structure may be the reason of the adsorption and aggregation of the platelets on the gel surface.

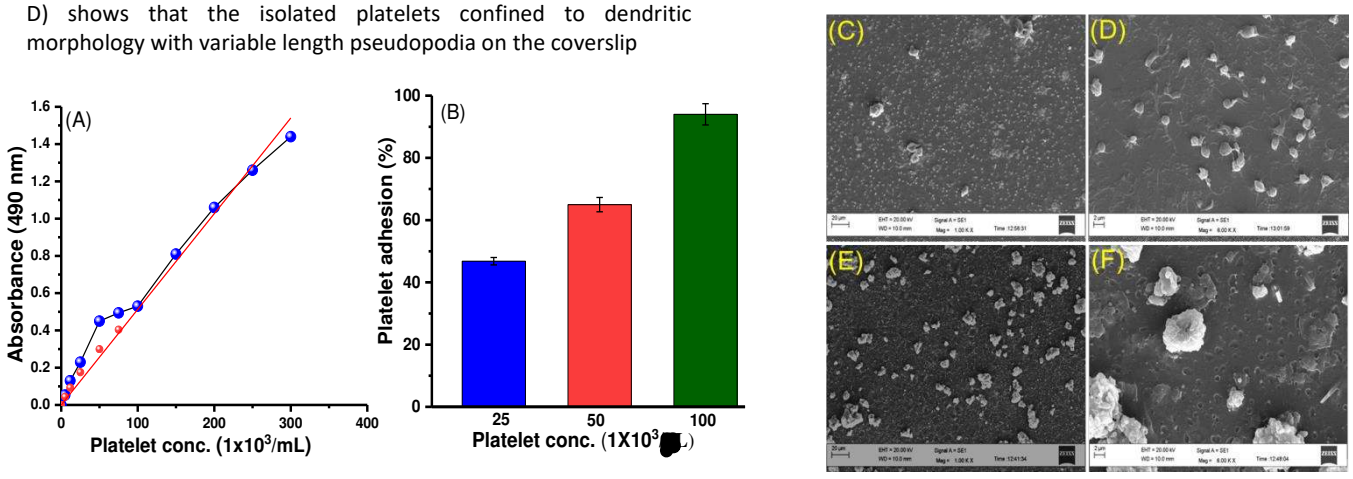

Figure 5. Affinity of a representative HG-2 hydrogel towards freshly isolated human platelets. Plot A: platelet adhesion assay to assess the platelet density on the hydrogel. Red line: ideal linear regression, black line with blue dots: defined platelet concentrations, red dots:

Journal of Materials Chemistry B

View Article Online
DOI: 10.1039/C7TB00848A

unknown platelet density on the gel. Bar diagrams: (B) calculated platelet adhesion. SEM images (two magnifications, 1.00 KX and 6.00 KX) of isolated human platelets adhered on coverslip (C and D) and HG-2 hydrogel (E and F).

After initial adhesion, platelets spread and gets activated in the presence of several agonists such as ADP and collagen. The activated platelets upon changes in the plasma membrane secrete LDH, transcription factors, and clotting factors. These enzymes were utilized to study the activation of platelets adhered on the gel. The resting platelets were considered control as they tend to release lesser LDH than activated platelets. LDH secreted from resting as well as activated platelets, both on the gel and the controls were measured. Two concentrations (50 x 10^3, 100 x 10^3 platelets/µL) of platelets were considered for the experiment. Adhered platelets on the hydrogel were markedly resting in comparison to standard platelets (Figure 6A). However in the presence of ADP, there was relative elevation in the LDH values. In such instance the gel could be previously formulated with ADP/collagen such that platelet activation gets more pronounced. Soon after the platelets are activated, and transcription factors are released, the thrombosis system gets activated, leads to the development of fibrin networks. The fibrin network co-initiates the reorganization process followed by platelet aggregation and coagulation. The fibrinogen adsorption activity of the hydrogel was determined to establish the fact that hydrogel can be used for healing the blood loss during vascular injury.

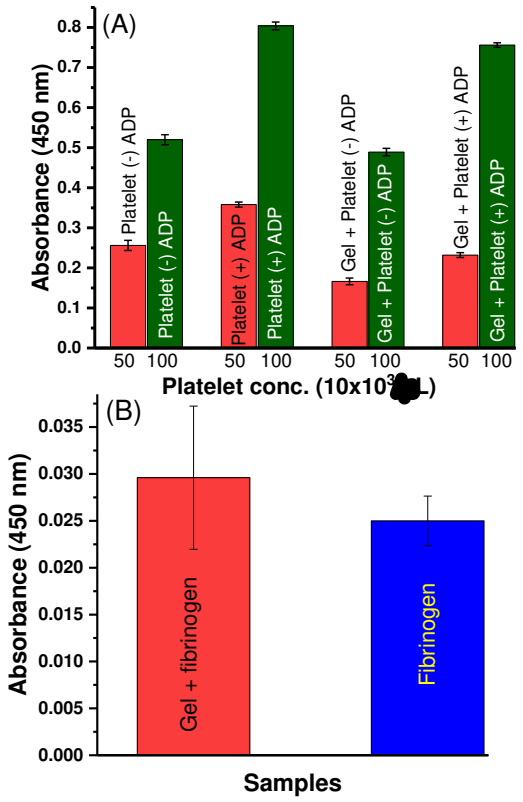

Figure 6. (A) platelet activation before and after ADP stimulation, and (D) fibrinogen adsorption by ELISA test showing relative fibrinogen adsorption on the HG-2 hydrogel and polystyrene plate (control) respectively (mean ± SD, n=3).

ELISA assay revealed increase in fibrinogen adsorption on the hydrogel (Figure 6B) as compared to control sample (fibrinogen on polystyrene 96 wells plate). This result also consistent with the SEM images of Figure 5 (images E and F). Based on the above experiments, the hydrogel appears to be potential in the cascade of tissue responses during injury.

Conclusion

We have successfully developed a new and fully aqueous-based injectable system for dual gelation. The system was based on rapid sequential nucleophilic substitution reaction between PEG containing activated chloride termini and poly[(2-dimethylamino)ethyl methacrylate]-*b*-poly(N-isopropyl acrylamide) copolymer. The main advantages of our injectable hydrogels are that the reaction is mild, necessarily avoids side reaction, and can be performed well below the physiological temperature with temperature rise as low as ca. 1 °C/g of injectable solution. Performing gelation below the physiological temperature is beneficial for administration of the gel which will avoid the adverse effect of temperature rise if any. High gel fraction after injection in the physiological conditions reveals good efficiency of our hydrogels. The hydrogels were chemically crosslinked and showed hardening effect at physiological temperature. The hydrogels exhibited tuneable degradation, pH and temperature responsive property, hemocompatibility and live cell viability. Cell proliferation with time and platelets adhesion/aggregation as well as fibrinogen adsorption ability make these hydrogels suitable for healing of wounds, and use in tissue regeneration. Our future work will deal with the elastic and crystalline hydrogels for tissue regeneration.

†Electronic supplementary information (ESI)

Experimental details for the synthesis of block copolymers, characterization of copolymers by 1H NMR, GPC, characterizations of hydrogels by ^{13}C NMR and FT-IR, evaluation of swelling behaviour, sol fraction, determination of temperature change during gelation, hemocompatibility, cytocompatibility, and adhesion of platelets on hydrogel by SEM.

Acknowledgments

CSIR-CSMCRI Registration No. 020/2017. This work is supported by Science & Engineering Research Board (SERB, project grant number EMR/2015/000843), Department of Science and Technology, Government of India. AKSC and NB thank CSIR, India for providing a research fellowship. We are grateful to Centralized Analytical Facility-CSMCRI for instrumental support. DK would also like to acknowledge the support provided by Shiv Nadar University, India and the technical support by Dr. Ruchita Pal for SEM imaging at Advanced Instrumentation Research Facility of JNU, India.

References

1. R. H. Schmedlen, K. S. Masters and J. L. West, *Biomaterials*, 2002, **23**, 4325-4332.
2. L. Cao, B. Cao, C. Lu, G. Wang, L. Yu and J. Ding, *J. Mater. Chem. B*, 2015, **3**, 1268-1280.
3. K. H. Bae, L. S. Wang and M. Kurisawa, *J. Mater. Chem. B*, 2013, **1**, 5371-5388.
4. S. Yan, X. Zhang, K. Zhang, H. Di, L. Feng, G. Li and J. Yin, *J. Mater. Chem. B,* 2016, **4**, 947-961.
5. D. R. Griffin, W. M. Weaver, P. O. Scumpia, D. Di Carlo and T. Segura, *Nature materials*, 2015, **14**, 737-744.
6. X. Zhao, H. Wu, B. Guo, R. Dong, Y. Qiu and P. X. Ma, *Biomaterials*, 2017, **122**, 34-47.
7. L. Sun, S. Zhang, J. Zhang, N. Wang, W. Liu and W. Wang, *J. Mater. Chem. B*, 2013, **1**, 3932-3939.
8. J. Hoque and J. Haldar, ACS Appl. Mater. Interfaces, DOI: 10.1021/acsami.7b03208.

9. C. Gong, Q. Wu, Y. Wang, D. Zhang, F. Luo, X. Zhao, Y. Wei and Z. Qian, *Biomaterials*, 2013, **34**, 6377-6387.

10. A. GhavamiNejad, C.H. Park and C.S. Kim, *Biomacromolecules*, 2016, **17**, 1213-1223.

11. N. Ninan, A. Forget, V.P. Shastri, N.H. Voelcker and A. Blencowe, *ACS Appl. Mater. Interfaces*, 2016, **8**, 28511-28521.

12. B. Jeong, Y. H. Bae, D. S. Lee and S.W. Kim, *Nature*, 1997, **388**, 860-862.

13. R. Censi, P. Di Martino, T. Vermonden, and W. E. Hennink, *J. Controlled Release*, 2012, **161**, 680-692.

14. T. Vermonden, R. Censi and W.E. Hennink, *Chemical Reviews*, 2012, **112**, 2853-2888.

15. A. S. Hoffman, *Adv. Drug Delivery Rev*., 2012, **64**, 18-23.

16. J. Liu, C. Qi, K. Tao, J. Zhang, J. Zhang, L. Xu, X. Jiang, Y. Zhang, L. Huang, Q. Li and H. Xie, *ACS Appl. Mater. Interfaces*, 2016, **8**, 6411-6422.

17. P. Davoodi, W. C. Ng, W. C. Yan, M. P. Srinivasan and C. H. Wang, *ACS Appl. Mater. Interfaces*, 2016, **8**, 22785-22800.

18. B. B. Seo, J. T. Koh and S. C. Song, *Biomaterials*, 2017, **122**, 91-104.

19. H. Wu, S. Liu, L. Xiao, X. Dong, Q. Lu and D. L. Kaplan, *ACS Appl. Mater. Interfaces* 2016, **8**, 17118-17126.

20. T. N. Vo, S. R. Shah, S. Lu, A. M. Tatara, E. J. Lee, T. T. Roh, Y. Tabata and A. G. Mikos, *Biomaterials*, 2016, **83**, 1-11.

21. A. K. Ekenseair, K. W. Boere, S. N. Tzouanas, T. N. Vo, F. K. Kasper and A. G. Mikos, *Biomacromolecules*, 2012, **13**, 1908-1915**.**

22. B. H. Lee, B. West, R. McLemore, C. Pauken and B. L. Vernon, *Biomacromolecules*, 2006, **7**, 2059-2064.

23. T. N. Vo, A. K. Ekenseair, F. K. Kasper and A. G. Mikos, *Biomacromolecules*, 2013, **15**, 132-142.

24. K. W. Boere, B. G. Soliman, D. T. Rijkers, W. E. Hennink and T. Vermonden, *Macromolecules*, 2014, *47*, 2430-2438.

25. H. G. Schild, *Prog. Polym. Sci.*, 1992, **17**, 163-249.

26. X. Zhao, B. Guo and P. X. Ma, *J. Mater. Chem. B*, 2015, **3**, 8459-8468.

27. S. J. Bae, J. M. Suh, Y. S. Sohn, Y. H. Bae, S. W. Kim and B. Jeong, *Macromolecules*, 2005, **38**, 5260-5265.

28. B. Jeong, L. Wang and A. Gutowska, *Chem. Commun.,* 2001, **16**, 1516-1517.

29. C. K. Han and Y. H. Bae, *Polymer*, 1998, **39**, 2809-2814.

30. B. Jeong, Y. H. Bae and S. W. Kim, *J. Controlled Release*, 2000, **63**, 155-163.

31. B. Jeong, S. W. Kim and Y. H. Bae, *Adv. Drug Delivery Rev.,* 2012, **64**, 154-162.

32. J. C. Garbern, A. S. Hoffman, and P. S. Stayton, *Biomacromolecules*, 2010, **11**, 1833-1839.

33. Y. Cheng, C. He, J. Ding, C. Xiao, X. Zhuang and X. Chen, *Biomaterials***,** 2013, **34**, 10338-10347.

34. L. Li, J. Gu, J. Zhang, Z. Xie, Y. Lu, L. Shen, Q. Dong and Y. Wang, *ACS Appl. Mater. Interfaces*, 2015, **7**, 8033-8040.

35. K. M. Galler, L. Aulisa, K. R. Regan, R. N. D'Souza and J. D. Hartgerink, *J. Am. Cem. Soc*., 2010, **132**, 3217-3223.

36. R. M. Schweller and J. L. West, *ACS Biomater. Sci. Eng*., 2015, **1**, 335-344.

37. K. Kushiro, T. Sakai and M. Takai, *Langmuir*, 2015, **31**, 10215-10222.

38. J. A. Burdick, A. J. Peterson and K. S. Anseth, *Biomaterials*, 2001, **22**, 1779-1786.

39. A. K. S. Chandel, A. Bera, B. Nutan and S.K. Jewrajka, *Polymer*, 2016, **99**, 470-479.

40. B. Nutan, A. K. S. Chandel, D. V. Bhalani and S.K. Jewrajka, *Polymer*, 2017, **111**, 265-274.

41. A. K. S. Chandel, C. U. Kumar and S. K. Jewrajka, *ACS Appl. Mater. Interfaces*, 2016, **8**, 3182-3192.

42. A. Bera, A. K. S. Chandel, C. U. Kumar, S. K. Jewrajka, *J. Mater. Chem. B*, 2015, **3**, 8548-8557

43. N. Pereira-Rodrigues, P. E. Poleni, D. Guimard, Y. Arakawa, Y. Sakai and T. Fujii, *PloS one*, 2010, **5**, 9667.

44. R. C. H. I. E. McNICOL, (SP Watson, KS, Authi eds), *Oxford: Oxford Univ, Press*, 1996 1-26.

45. S. Braune, S. Zhou, B. Groth and F. Jung, *Clin. Hemorheol. Microcirc.,* 2015, **61**, 225-236.

46. B. A. Butruk-Raszeja, I. Lojszczyk, T. Ciach, M. Koscielniak-Ziemniak, K. Janiczak, R. Kustosz and M. Gonsior, *Colloids Surf. B,* 2015, **130**, 192-198.

47. N. Bhingaradiya, A. K. S. Chandel and S. K. Jewrajka, *Chem. Eur. J.* 10.1002/chem.201701900.

48. G. Kali, S. Vavra, K. Laszlo and B. Ivan, *Macromolecules*, 2013, **46**, 5337-5344.

49. S. Kim, K. Lee and C. Cha, *J. Biomater. Sci. Polym. Ed*., 2016, **27**, 1698–1711.

50. P. Van de Wetering, N. J. Zuidam, M. J. Van Steenbergen, O. A. G. J. Van der Houwen, W. J. M. Underberg and W. E. Hennink, *Macromolecules*, 1998, **31**, 8063-8068.

51. J. F. Krzyzaniak, F. A. A. Nuunnez, D. M. Raymond and S. H. Yalkowsky, *J. Pharm. Sci.,* 1997, **86**, 1215-1217.

52. Z. M. Ruggeri, *Microcirculation*, 2009, **16**, 58-83.

View Article Online
DOI: 10.1039/C7TB00848A

Table of Content

Series of poly(ethylene glycol)-based dually crosslinked bioderadable/biocompatible injectable hydrogels have been developed through extremely simple chemistry which avoids use of small molecular weight crosslinker, formation of by-products and involved low heat change. The hydrogels are useful for deep wound healing and soft tissue regeneration.